Int. J. Solids Structures Vol. 22, No. 7, pp. 833–843, 1986
Printed in Great Britain.

0020-7683/86 $3.00 + .00
Pergamon Journals Ltd.

THREE-DIMENSIONAL FINITE ELEMENT SIMULATION OF POST-YIELD FRACTURE EXPERIMENTS

W. SCHMITT
Fraunhofer-Institut für Werkstoffmechnik, Wöhlerstr. 11, 7800 Freiburg, Federal Republic of Germany

(*Received* 30 *April* 1985)

Abstract—It is shown that the evaluation of the *J*-integral by the virtual crack extension method gives "path-independent" results and is equivalent for 2D problems to the contour-integral evaluation also with significant load relief due to crack extension, provided the stress work density W is defined appropriately. Despite encouraging results concerning the application of 3D finite element procedures to complex structures there remains the problem to quantify the influence of the local stress state on the material resistance against crack propagation.

THE *J*-INTEGRAL CONCEPT

Several concepts have been proposed to describe the process of crack initiation and propagation in ductile materials. Every concept assumes a suitable loading parameter L, which characterizes the intensity of the stress and strain field in a relevant vicinity of the crack front. The onset of crack extension takes place if L exceeds a critical material value L_c. If stable crack extension occurs it is controlled by the respective material resistance curve $L(\Delta a)$. Beside the crack tip opening displacement CTOD the so-called *J*-integral has obtained wide acceptance as a fracture parameter in the ductile regime.

Path-independent integrals for two-dimensional crack problems were introduced independently by Cherepanov[1] and Rice[2]. Rice's work especially gave significant impulses towards the application of the *J*-integral

$$J = \oint_\Gamma \left(W \, \mathrm{d}y - T_i \frac{\partial u_i}{\partial x} \mathrm{d}s \right) \tag{1}$$

to fracture problems where linear elastic fracture mechanics LEFM is no longer valid. He could also demonstrate that J is equivalent to the energy release rate

$$J = -\frac{\partial U}{\partial A}, \tag{2}$$

if elastic (linear or non-linear) material behaviour is assumed with

W	strain energy density
Γ	integration path around the crack tip
s	arc length on Γ
n_j	components of the unit outward normal vector on Γ
σ_{ij}	components of the stress tensor
$T_i = \sigma_{ij} n_j$	components of the traction vector
u_i	components of the displacement vector
U	potential energy
p_i	external force vector
V	volume
A	crack area
ε_{ij}	components of the strain tensor.

This latter interpretation of J served as basis for test procedures to measure the material fracture toughness J_{Ic}. So, Begley and Landes[3] proposed a multi-specimen procedure to

experimentally determine the energy release rate, which is exact if the material can be described by a deformation plasticity. To avoid principal difficulties arising from a multi-specimen test procedure, Rice *et al.*[4] proposed estimation techniques for J from a single load–displacement record.

If the material is sufficiently ductile a structure will not fail immediately if the crack tip loading parameter J reaches the initiation value J_i, but there may be stable crack extension with still increasing load and increasing J. This behaviour is characterized by the J-resistance curve $J(\Delta a)$. To measure this material resistance curve the crack driving parameter J and the crack extension Δa must be evaluated. Clarke *et al.*[5] proposed the partial unloading technique which allows to determine the amount of crack extension in the course of a single specimen experiment by repeated small unloadings using elastic compliance calculations. In two-dimensional cases the numerical evaluation of J is readily available by using (1) at the end of a finite element or finite difference analysis. More efficient for finite element applications and easily extended to three-dimensional situations is the stiffness derivative method introduced by Parks[6] for elastic and elastic-plastic situations. DeLorenzi[7] introduced a node shifting and releasing technique to model crack extension for plane problems.

The application of these experimental and numerical procedures based on (2) is certainly valid also for materials described by an incremental law of plasticity if the loading of the structure is proportional with no unloadings anywhere in the structure. This condition is violated if crack extension takes place. The possible error was considered tolerable if the relative amount of crack extension was small compared with specimen dimensions.

The theoretical basis of the J-concept can be found by consideration of conservation laws within the theory of elasticity. So, for instance, Eshelby[8–10] found that the force on a defect in linear elastic continua can be expressed as a surface integral of the energy momentum tensor. Buggisch *et al.*[11] generalized these considerations and took also nonmechanical dissipative energy terms into account. By neglecting dissipative terms and volume forces, by assuming static cases and a "hyperelastic" material for which the stresses can be derived from a potential

$$\sigma_{ij} = \frac{\partial W}{\partial \varepsilon_{ij}} \tag{3}$$

they were able to obtain (1) as a special case of their formulation.

At this point it is important to note that (3) does not necessarily imply elastic material behaviour. For a material described by an incremental law of plasticity, i.e. the unloading path is different from the loading path, the stress work density is defined in analogy to the elastic case.

$$W = \int_0^{\varepsilon_{ij}} \sigma_{ij}\, \mathrm{d}\hat{\varepsilon}_{ij}. \tag{4}$$

From (4) follows immediately that (3) holds for any time in the loading history. It is important to note that in the general elastic-plastic case W is no longer a unique function of the stresses and strains only. However, W contains all dissipative terms coming from plasticity. It must be integrated over the loading history, which will usually require numerical analyses.

In conclusion it may be stated that also for elastic-plastic material behaviour J is equivalent to the variation of the potential U with respect to virtual crack extension

$$J = -\frac{\partial U}{\partial A} \tag{5}$$

with W according to (4) and

$$U = \int_V (W - p_i u_i)\, \mathrm{d}V. \tag{6}$$

J no longer has the meaning of a (recoverable) energy release rate. Instead, J is dominated by dissipative plastic work terms. This reflects the fact that in ductile materials initiation and propagation of a crack requires a significant volume around the crack tip to be plastically deformed. If the structure is loaded to the plastic collapse load, J may increase without further increase of the load. From this steep increase of J the plastic collapse load for arbitrarily loaded structures can be evaluated by using the J-integral. Having in mind that in the brittle material regime J is correlated with K it may be stated that the J-concept covers the whole range of material behaviour from linear elastic fracture mechanics to plastic collapse.

If all quantities entering (5) and (6) are known the according J can be uniquely determined, although it is in general dependent on the load history. On the other hand, J defines the stress–strain around the crack front uniquely only in certain limiting cases. How much this fact prohibits the application of the J-concept in engineering practice and if the introduction of an additional parameter controlling the degree of tri-axiality or constraint will bring about the necessary improvements must still be examined. The observed variation of J-resistance curves for different specimen geometries leads to the assumption that the influence of the constraint needs further investigations. It should be noted here that these problems are not specific with the J-concept but arise in all elastic-plastic fracture concepts discussed in the literature.

Through (5) the application of the stiffness derivative method is possible also for the numerical simulation of J-controlled crack growth in steels described by an incremental theory of plasticity and with unloading occurring in parts of the structure.

NUMERICAL RESULTS

At the IWM, the possibilities to calculate the J-integral by the stiffness derivative procedure and to model crack propagation in 2D and 3D situations have been implemented into the commercial finite element program ADINA[12] and successfully applied to elastic-plastic crack problems[13–16]. Through appropriate correction terms "path independence" is maintained also for non-isothermal and dynamic cases or if the crack surfaces are loaded by pressure. In Ref. [13] two-dimensional finite element analyses of a side-grooved compact specimen were performed to generate fictitious force displacement records for different $J(\Delta a)$-curves. The analysis with the flattest $J(\Delta a)$-curve has been reevaluated to verify the equivalence of J according to (1) and (5). Figure 1 shows the calculated J-values from the line integral (1) and from the stiffness derivative method (5). J is plotted vs force and vs displacement. Even though this analysis represents the most critical case from the numerical point of view, up to the total amount of crack propagation of 20% of the ligament there is no numerical difference between the two evaluations. Only when the crack tip is no longer surrounded by the integration paths or areas the calculated values become meaningless and show increasing discrepancies. The crack propagation associated with the largest load point displacement in Fig. 1 was about 40% of the original ligament.

To investigate the problem of transferability of J-resistance curves an attempt was made to predict the behaviour of a smooth specimen by applying a $J(\Delta a)$-curve from a side-grooved specimen. For this study two specimens (thickness $B = 25$ mm) were taken from the same plate (steel A 542, yield stress and ultimate strength 533 MPa and 670 MPa, room temperature) at adjacent locations in the same orientation. The first specimen had 20% side-grooves, the second specimen was tested without side-grooves and consequently showed significant tunnelling of the crack front, as can be seen from Fig. 2. The force–displacement curves and the J–R curves from the experiments are given in Figs. 3 and 4. More details about the experiments are given in [17].

To demonstrate the capability of the numerical method the first experiment was analysed in two dimensions. A relatively fine mesh with 96 elements and a total of 334 nodal points was used. The crack tip was modelled with conventional four-sided elements in plane strain. The crack growth rate was controlled via the measured displacement versus crack growth curve. To transfer results from specimens to real components the simulation must be controlled by a J–R curve. Also, the numerical effort needed to perform such kind

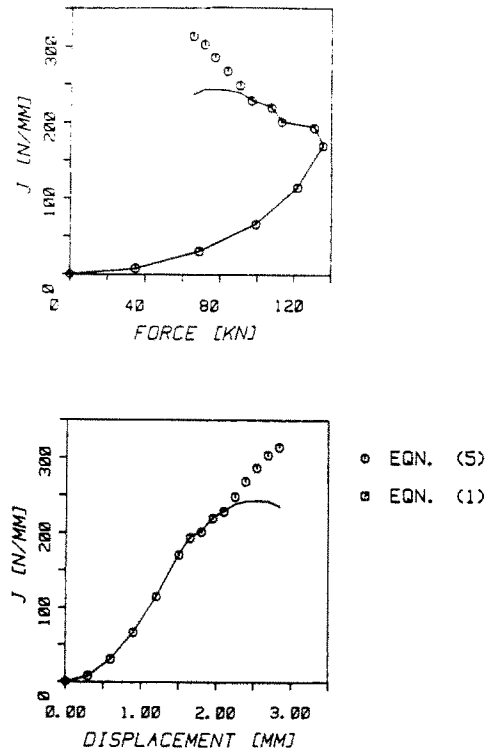

Fig. 1. Comparison of J vs force and J vs displacement calculated from the line integral (1) and from the stiffness derivative method (5).

of analysis is still very high and all possibilities must be examined to reduce this effort. This is especially important if one considers applications in three dimensions. Therefore, a parameter study has been performed where the finite element meshes have been simplified to only 32 elements and the control of the simulation by a material J–R curve has been incorporated. Figure 5 shows the force displacement diagrams of the experiment and of the numerical simulations. The forces per unit thickness of the numerical simulation have been multiplied by the net thickness of the specimen to obtain the total force to be compared with the experiment. The agreement between the experiment and the numerical simulations is good.

In the case of side-grooved specimens a two-dimensional analysis in plane strain seems to predict the behaviour of global parameters force, displacement and also the J-integral with sufficient accuracy. For the smooth specimen the fatigue crack front and especially the crack front after stable crack extension is not straight at all (Fig. 2). So, a three-dimensional finite element analysis of this experiment has been performed under the following restrictions.

To simplify the set-up of the original finite element mesh a straight initial crack front was assumed with $a = 30$ mm as opposed to the real crack front with $a_{max} = 30.2$ mm, $a_{min} = 28.8$ mm and an average of $a = 29.8$ mm. The local crack extension in the simulation is controlled by comparing local values of J (eqn 5) at four positions along the (half-) crack front with the J-resistance curve of the side-grooved specimen tested at the same temperature. Figure 6 shows this J–R curve together with the two-dimensional simulation.

The finite element model (Fig. 7) consists of 66 elements with 20 nodes each, amounting to a total of 1260 degrees of freedom. In every layer a ring of 5 collapsed elements is arranged around the crack front. Multiple crack tip nodes and the mid-side position of the mid-side nodes ensure a r^{-1}-singularity in the strains. The loading of the specimen is simulated by imposing constant displacement increments along a line representing the bolts. For reasons of symmetry only one quarter of the specimen is modelled. A total of 10 displacement increments was used. Figure 8 shows the force–displacement diagrams of the

Fig. 2. Crack surface of the smooth specimen.

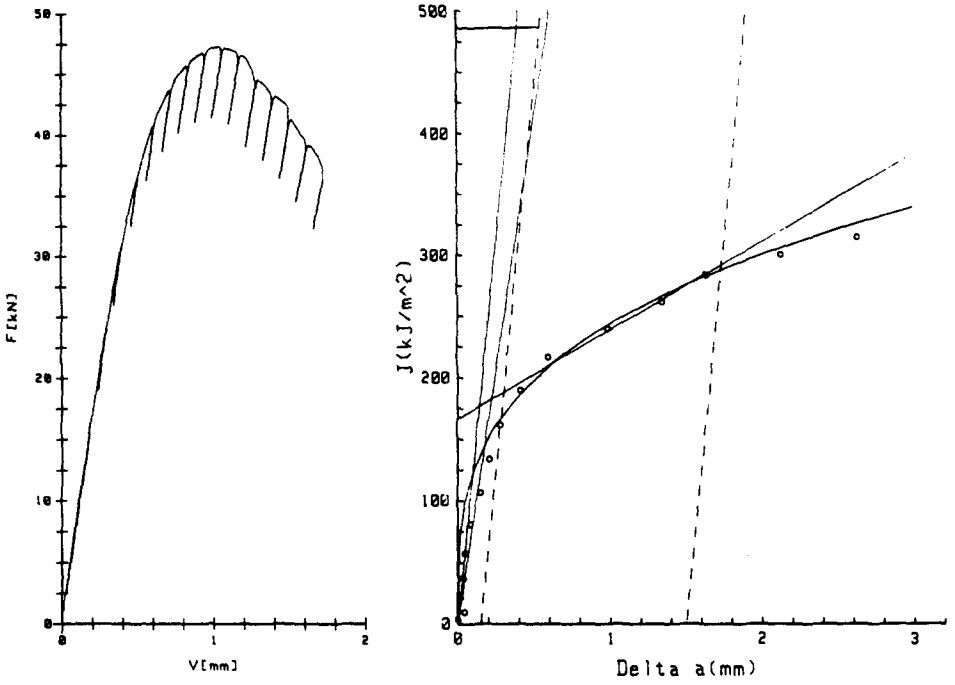

Fig. 3. F vs V diagram at room temperature and related J–R curve (20% side-grooves).

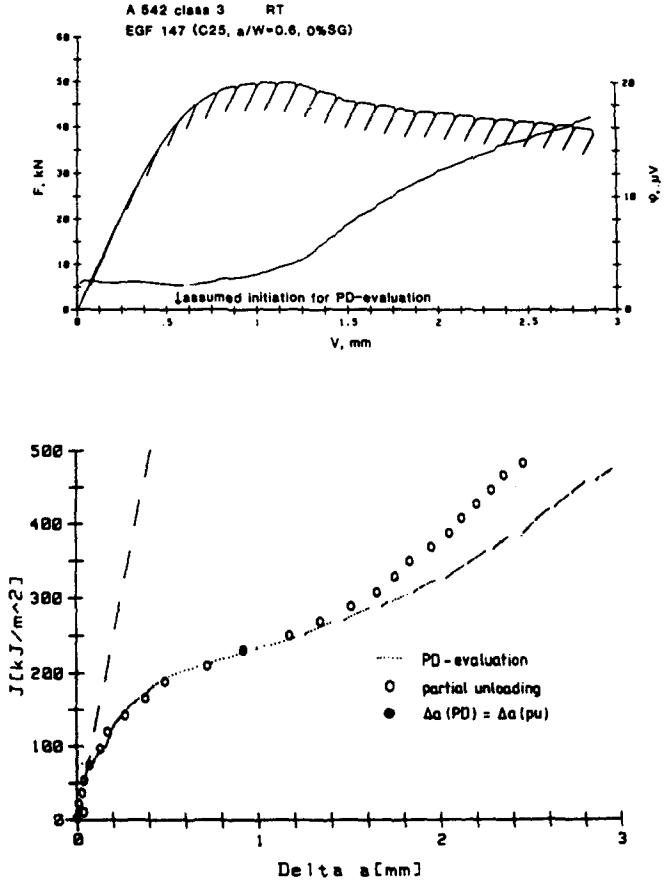

Fig. 4. F vs V diagram at room temperature and related J–R curve (smooth specimen).

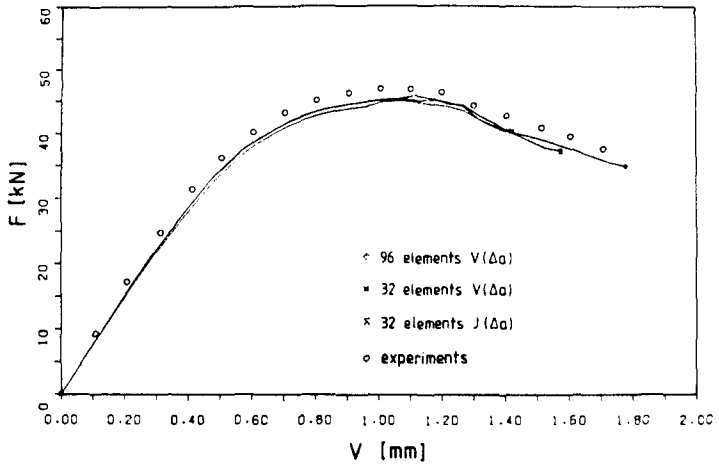

Fig. 5. Convergence study plane strain, F vs V diagrams.

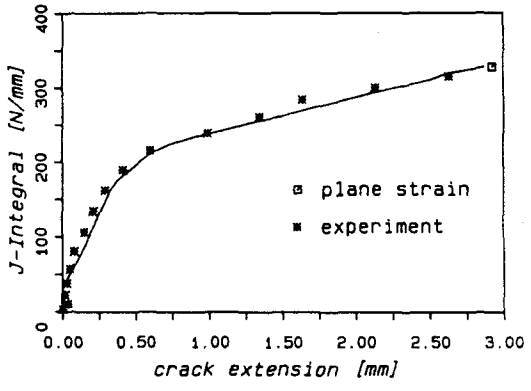

Fig. 6. J–R curves, plane strain simulation and experiment (20% side-grooves).

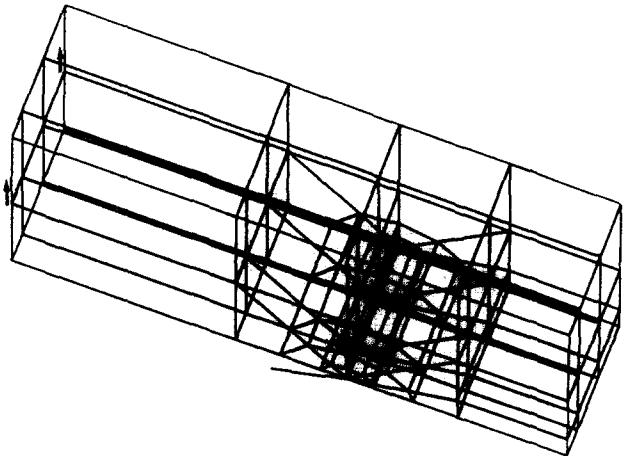

Fig. 7. Finite element model 3D.

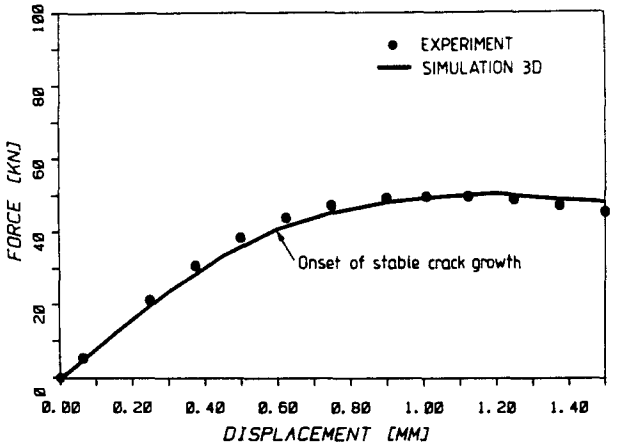

Fig. 8. F vs V diagram, 3D-simulation and experiment (smooth specimen).

experiment and the simulation. Despite the complexity of the experiment and the limitations in the model, the agreement is good.

The evaluation of the local values of J along the crack front according to eqn (3) is shown in Fig. 9 for different load-line-displacements. After step 4 or $V = 0.6$ mm respectively the initiation value J_i is exceeded in the middle of the specimen and the crack starts to propagate in the model. The calculated shape of the crack front is plotted in Fig. 10. Note that the crack shape is adjusted after each load step according to the J-variation of the previous load step. The simulation predicts very well the tunnelling of the crack front in the middle of the specimen. It overestimates, however, the crack propagation at the surfaces. In the experiment no crack extension was observed at the surfaces even for much higher displacements than $V = 1.5$ mm where this analysis was terminated.

In Fig. 11 the average value of J is plotted vs the average value of crack propagation and compared with the experimental evaluation. There is significant deviation between the two curves. The first obvious reason might be that the single J–R curve taken from the first specimen does not represent the material at the location of the second specimen. Moreover, due to the fact that a resistance curve obtained from a side-grooved specimen was used to control crack growth in the smooth specimen the influence of the constraint was not taken into account. As can be concluded from the prediction of the crack extension at the surface, the simulation certainly overestimates the crack propagation. On the part of the experiments no direct information of the crack shapes was available in the course of the test. The average

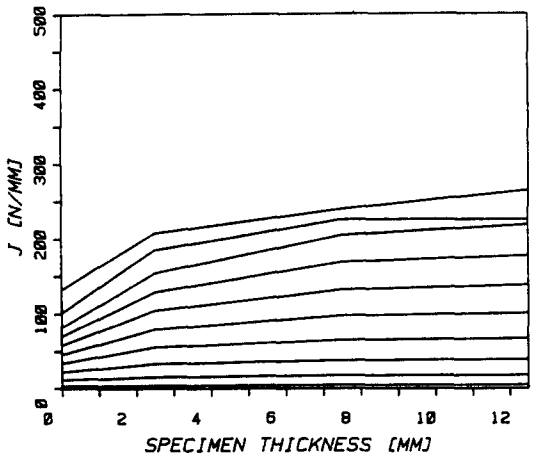

Fig. 9. J-Integral across the specimen thickness.

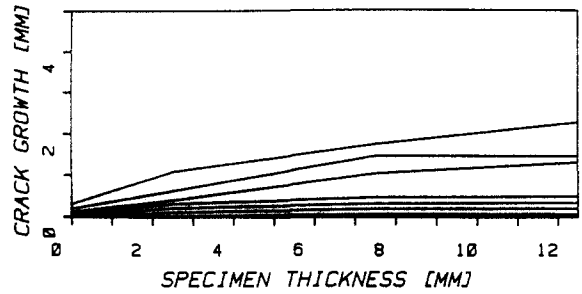

Fig. 10. Shape of the crack front.

crack growth was rather concluded from the unloading compliance. For the final crack shape the unloading compliance significantly under-estimated the average crack length. It is not clear, however, whether this effect is also present for the relatively small crack extensions plotted in Fig. 11. If so, the experimental curve would come down, while the simulated J–R curve would come up for reasons mentioned above.

To gain some insight into the variation of the constraint along the curved crack front the ratio of the tangential stress component over the sum of the in-plane components (times the Poisson's ratio) is plotted over the specimen thickness in Fig. 12 for integration points close to the ligament directly ahead of the crack front. The evaluation was done for the final (10th) load step. The upper curve is obtained with $\nu = 0.3$, the lower curve with $\nu = 0.5$. The solid line is obtained using the principal stresses, the crosses mark the respective values, if the x-, y- and z-components are used instead. Although no quantitative explanation of this ratio, which should be unity for linear elastic material and plane strain, can be given for elastic-plastic material behaviour, the trend clearly indicates a significant decrease of the tri-axiality when the surface is approached. This corresponds to an increase in the material resistance at the surface which can explain the fact that in the experiment the crack did not even initiate at the surface.

CONCLUSIONS

The evaluation of the J-integral by the virtual crack extension method gives "path-independent" results and is equivalent for 2D-problems to the contour-integral evaluation also if significant load relief takes place in an elastic-plastic material.

Three-dimensional finite element procedures including the modelling of stable crack propagation were applied to predict the behaviour of a smooth specimen from a J–R curve measured on a side-grooved specimen. The results are very encouraging with respect to the

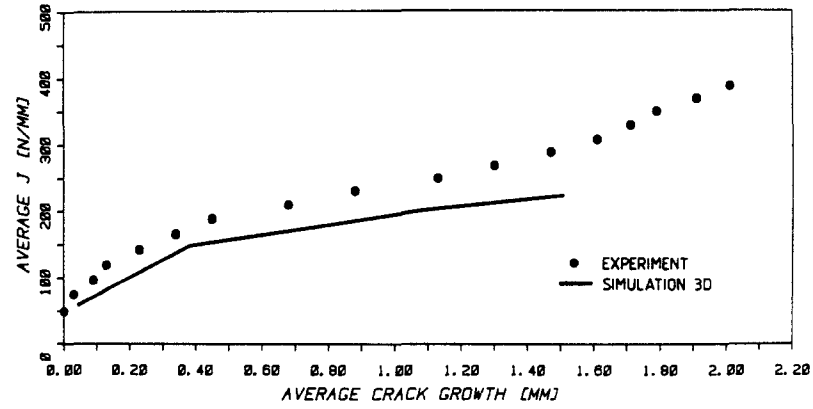

Fig. 11. Comparison of J–R curves.

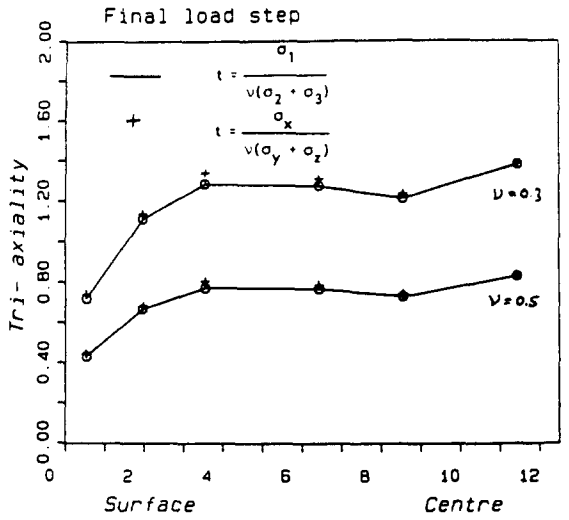

Fig. 12. Variation of constraint along crack front.

force–displacement curve of the specimen. For reasons given above, the agreement of analysis and experiment in the near-crack-tip behaviour and in the global J–R curve is only qualitative.

To proceed further in the question of transferability, more experimental and numerical work is necessary, especially to quantify the influence of the stress state on the resistance of a material against crack initiation and propagation.

Acknowledgement—The author is grateful to the Bundesminister für Forschung und Technologie, who supported the major part of this work under project number 150 488.

REFERENCES

1. G. P. Cherepanov, Crack propagation in continuous media. *J. Appl. Math. Mech.* (PMM) **31**, 476–485 (1967).
2. J. R. Rice, A path independent integral and the approximate analysis of strain concentrations by notches and cracks. *J. Appl. Mech.* **35**, 379–386 (1968).
3. J. A. Begley and J. D. Landes, In *Fracture Toughness*, ASTM STP 514, pp. 1–20. American Society for Testing and Materials (1972).
4. J. R. Rice, P. Paris and J. G. Merkle, In *Progress in Flaw Growth and Fracture Toughness Testing*, ASTM STP 536, pp. 231–245. American Society for Testing and Materials (1973).
5. G. A. Clarke, W. R. Andrews, P. C. Paris and D. W. Schmidt, In *Mechanics of Crack Growth*, ASTM STP 590, pp. 27–42. American Society for Testing and Materials (1976).
6. D. M. Parks, The virtual crack extension method for nonlinear material behaviour. *Comp. Methods Appl. Mech. Engng* **12**, 353–364 (1977).
7. H. G. DeLorenzi, J-integral and crack growth calculations with the finite element program ADINA, Methodology for plastic fracture, EPRI Report SRD-78-124 (1987).
8. J. D. Eshelby, The force on an elastic singularity. *Phil. Trans. R. Soc. London A* **244**, 87–112 (1951).
9. J. D. Eshelby, Energy relations and energy-momentum tensor in continuum mechanics. In *Inelastic Behaviour of Solids* (Edited by Kanninen *et al.*), pp. 77–115. New York (1970).
10. J. D. Eshelby, The calculation of energy release rates. In *Prospects of Fracture Mechanics* (Edited by G. C. Sih *et al.*), pp. 69–84. Leyden (1975).
11. H. Buggisch, D. Gross and K. H. Krüger, Einige Erhaltungssätze der Kontinuumsmechanik vom J-Integral-Typ. *Ing. Arch.* **50**, 103–111 (1981).
12. K.J. Bathe, ADINA, a finite element program for automatic dynamic incremental nonlinear analysis, Report 82 448-1, Massachusetts Institute of Technology, Cambridge, MA (1980).
13. W. Schmitt and B. Voß, Numerical simulation of post yield fracture experiment as a basis for the transferability to components. *Nucl. Engng Design* **76**, 319–328 (1983).
14. D. Siegele and W. Schmitt, Determination and simulation of stable crack growth in ADINA. *Int. J. Comp. Structures* **17**, 697–703 (1983).
15. D. Siegele, H. Kordisch and W. Schmitt, J-Integral-Berechnung für rißbehaftete Strukturen unter Temperatur- und Innendruckbelastung, 16. Sitzung des Arbeitskreises Bruchvorgänge im DVM, Karlsruhe (1984).
16. W. Schmitt, Three-dimensional finite element simulation of post-yield fracture experiments. In *Computational Fracture Mechanics—Nonlinear and 3-D Problems*, PVP **85**, AMD **61**, 119–131 (1984).
17. B. Voß and R. A. Mayville, On the use of partial unloading compliance method for the determination of J–R-curves and J_{Ic}, Symposium on Users Experience with Elastic-Plastic Fracture Toughness Test Methods, Louisville, KY, April 1983, to be published in ASTM STP.